DOI: 10.1002/((please add manuscript number))
Article type: Communication

Bis-tridentate Ir(III) Metal Phosphors for Efficient Deep-Blue Organic Light-Emitting Diodes

Hsin-Hung Kuo,[a,‡] Yi-Ting Chen,[b,‡] Leon R. Devereux,[c,‡] Chung-Chih Wu,[b,] Mark A. Fox,[c,]* Chu-Yun Kuei,[a] Yun Chi,[a,]* and Gene-Hsiang Lee[d]*

[a] Department of Chemistry, National Tsing Hua University, Hsinchu 30013, Taiwan; E-mail: ychi@mx.nthu.edu.tw

[b] Graduate Institute of Electronics Engineering and Department of Electrical Engineering, National Taiwan University, Taipei 10617, Taiwan; E-mail: wucc@ntu.edu.tw

[c] Department of Chemistry, Durham University, South Road, Durham, DH1 3LE, UK; E-mail: m.a.fox@durham.ac.uk

[d] Instrumentation Center, National Taiwan University, Taipei 10617, Taiwan.

[‡] Authors with equal contribution.

Keywords: (iridium, phosphorescence, organic light emitting diode, carbene, pyrazole, tridentate)

Emissive Ir(III) metal complexes possessing two tridentate chelates (bis-tridentate) are known to be more robust compared to those with three bidentate chelates (tris-bidentate). Here, the deep blue-emitting, bis-tridentate Ir(III) metal phosphors bearing

both the dicarbene pincer ancillary such as 2,6-diimidazolylidene benzene and the 6-pyrazolyl-2-phenoxylpyridine chromophoric chelate, were synthesized. A deep-blue OLED from one phosphor exhibited $CIE_{(x,y)}$ coordinates of (0.15, 0.17) with maximum external quantum efficiency (max. EQE) of 20.7% and EQE = 14.6% at the practical brightness of 100 $cd \cdot m^{-2}$.

The third-row transition metal complexes are pivotal to the development of organic light-emitting diodes (OLEDs), which can be fabricated with unitary internal quantum efficiencies, attributed to the heavy-atom induced spin-orbital coupling that allow fast singlet-triplet intersystem crossing and efficient phosphorescence at RT.[1] However, the main barrier is the lack of stable and efficient blue-emitting phosphors, for which the developments still lag behind the green and red counterparts due to the intrinsically wider energy gaps.[2] Efficient blue-emitters are expected to reduce power consumption and improve color gamut; therefore, they have emerged as one paradigm of the full-color OLED displays and solid-state lighting.[3]

Among the various known blue phosphors, the sky-blue emitter FIrpic is considered to be the archetypal design; hence, its modulation is at the forefront of modern research in OLEDs.[4] OLEDs made with FIrpic typically have $CIE_{(x,y)}$ coordinates of (0.17, 0.34) which is far from the National Television Standards Committee (NTSC) pure blue values of (0.14, 0.08). Progress with blue phosphors is further complicated by other issues, such as chemical and physical stabilities, emission quantum yield and relative radiative lifetime. Moreover, almost all reports of decent blue phosphors were focused on the so-called tris-bidentate architectures, i.e. with either three bidentate cyclometalates of higher ligand-centered $\pi\pi^*$ energy gap or two of these cyclometalate plus a third bidentate ancillary.[5] However, these

complexes suffer from possible chelate dissociation upon excitation, giving inferior device performances and longevity.[6]

Recently, Williams,[7] Haga,[8] De Cola[9] and Esteruelas[10] have independently conducted studies on emitters bearing two tridentate chelates; namely bis-tridentate metal complexes. This class of molecular designs is expected to be more robust and should be of higher efficiency attributed to the concomitant higher rigidity vs. the traditional design bearing three bidentate chelates.[11] Despite the obvious advantages, these associated studies were greatly hampered by the lack of systematic syntheses and poor performances on OLEDs. These difficulties were recently solved by proper selection of chelates to give the charge-neutral architecture[12] and the instalment of a higher field strength coordination unit.[13]

One known bis-tridentate metal complex is the sky-blue Ir(III) phosphor [Ir(mimf)(pzpyph^{F})] (**SB** = 'sky-blue')[14] where the tridentate 6-pyrazolyl-2-phenylpyridine (pzpyph^{F}) and pincer dicarbene chelate (mimf) act as the chromophoric and ancillary chelates, respectively. These ligands control the emission color and give the greater ligand field strength needed for the efficient phosphors.[15] Hence, the OLED derived from **SB** gave maximum external quantum efficiency (max. EQE) of 27% and EQE of 24% at the practical brightness of 100 cd·m^{-2}. However, this device has CIE$_{(x,y)}$ coordinates of (0.18, 0.40) which is less satisfactory than OLEDs fabricated from FIrpic.

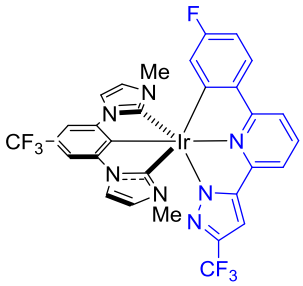

[Ir(mimf)(pzpyph^{F})]

(**SB**)

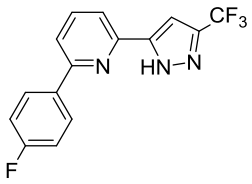

(pzpyph^{F})H$_2$

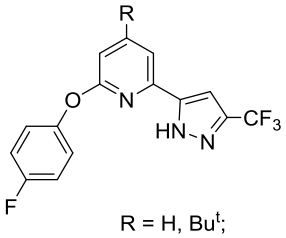

R = H, Bu^{t};

(pzpy^{R}Oph^{F})H$_2$

Both pyridyl and fluorophenyl units in the chromophoric chelate in this bis-tridentate Ir(III) phosphor **SB** had shown significant contributions to the frontier orbitals.[14] Thus, we decided to break the π-conjugation between the pyridyl and fluorophenyl units with the intention of widening the HOMO-LUMO energy gap (HLG) in our bis-tridentate Ir(III) template for a more blue emission.[16] The pzpyph^{F} chromophoric chelate[14] was deliberately replaced with the phenoxy-containing chelate (cf. pzpy^{R}Oph^{F}H$_2$, R = H, Bu^{t}) which proved to be simple to synthesize and can indeed be manipulated with various substituents if desired. Indeed, these new bis-tridentate Ir(III) phosphors have given deep blue emissions. As a proof-of-concept, they were applied in the fabrication of deep blue-emitting OLEDs, featuring comparable or an even better performance vs. the deep blue-emitting OLEDs based on traditional tris-bidentate Ir(III) metal phosphors.[17]

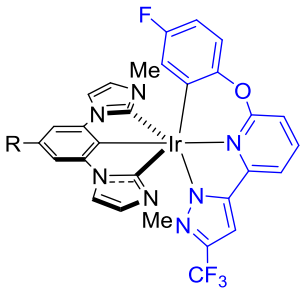

(**1**) [Ir(mimf)(pzpyOph^{F})], R = CF$_3$

(**2**) [Ir(mimb)(pzpyOph^{F})], R = Bu^{t}

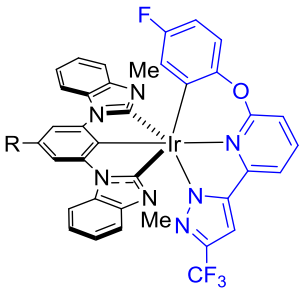

(**3**) [Ir(mbif)(pzpyOph^{F})], R = CF$_3$

(**4**) [Ir(mbib)(pzpyOph^{F})], R = Bu^{t}

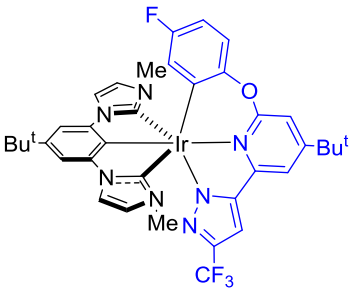

(**5**) [Ir(mimb)(pzpy^{Bu}Oph^{F})]

The pincer dicarbene ancillary chelate (e.g. 2,6-diimidazolylidene or 2,6-dibenzimidazolylidene benzene) is retained in the molecules for the higher metal-

chelate bond strength. Syntheses of blue-emitting Ir(III) metal complexes **1 - 5** required both tridentate pro-chelates i.e. monoanionic *bis*(imidazolylidene) benzene and dianionic 6-pyrazolyl-2-phenoxylpyridine. The pincer dicarbene chelate precursors are PF_6^- salts of $(mimf)H_3^{2+}$, $(mimb)H_3^{2+}$, $(mbif)H_3^{2+}$ and $(mbib)H_3^{2+}$ (Scheme S1) which were synthesized using literature procedures.[18] The dianionic chromophoric chelate precursors $(pzpy^{R}Oph^{F})H_2$, R = H and Bu^t, were prepared from Cu-catalyzed arylation of phenols[19] followed by Claisen condensation and hydrazine cyclization (Scheme S2).

The blue-emitting Ir(III) metal complexes **1 - 5** were successfully obtained by simply heating both pro-chelate precursors, with $IrCl_3 \cdot 3H_2O$ and KOAc in refluxing propionic acid (see ESI for details). This one-pot synthetic protocol offers much better product yields compared to the original procedures.[14] In the X-ray structure of $[Ir(mbib)(pzpyOph^{F})]$ **4** (Figure S1), the enlarged terminal-to-terminal bite angle of C-Ir-N = 168.25(14)° involving the $pzpyOph^{F}$ chelate suggests a reduced geometrical distortion compared to other Ir(III) complexes with 6-pyrazolyl-2-phenylpyridine chelates (~157°) and this distortion is believed to be beneficial to the increased ligand field strength and reduced quenching of the emission.[20]

The absorption spectra of all five Ir(III) complexes in CH_2Cl_2 solutions are depicted in Figure 1, while Table 1 lists the respective photophysical data. Complexes **3 - 4** exhibit more intense absorption peaks in the shorter wavelength region (260 ~ 350 nm) than other analogues due to the benzo substituents present in the pincer dicarbene chelate. The weaker absorption peaks occurring in the 350 to 430 nm region are attributed to the mixed singlet and triplet metal-to-ligand charge transfer (MLCT) transitions in all five complexes.

The five bis-tridentate Ir(III) metal complexes **1** - **5** show emission onsets at ~425 nm, peak maxima at ~472 nm, and two weak shoulders at ca. 448 and 505 nm and emission full width at half maxima (FWHM) of ~3330 - 3700 cm^{-1} (Figures 2 and Table 1). The very shifting of emission maxima implies that the substituents in these complexes have little effect on the emission color. The emission of **2** differs slightly from other Ir(III) complexes with a less structured profile and the peak maximum is red-shifted to 478 nm. All emission spectra of these complexes are clearly blue shifted vs. the emission spectrum for the Ir(III) reference **SB** as shown in Figure 2.

The high emission quantum yields (Φ) of all studied complexes **1** - **5** are fostered by the rigidified skeleton of the bis-tridentate architecture.[11] Their phosphorescent nature ($S_0 \leftarrow T_1$) is verified by the drastic oxygen quenching in aerated solution and long emission lifetime recorded upon degassing (Table 1). The observed emission lifetimes of **3** and **4** are found to be substantially longer than their counterparts **1** and **2** apparently due to the enhanced conjugation of the benzimidazolylidene (vs. imidazolylidene) fragments. This fused ring conjugation leads to a lowered electron density at the Ir(III) metal center and, hence, reduced MLCT character at the excited state. The reduced emission lifetimes for **2** and **5** (τ_{obs} = 4.4 and 8.7 μs) in CH_2Cl_2 at RT, indicate greater MLCT contributions in these complexes compared to **1**, **3** and **4** (τ_{obs} from 19 to 61 μs). Therefore, Ir(III) complexes **2** and **5** are considered to be the most suitable OLED emitters (for comparison, **SB** has an observed lifetime of 5.4 μs).

Cyclic voltammetry studies on **1** - **5** reveal reversible oxidation and irreversible reduction waves (Figure S2) with data summarized in Table 1. Complexes **1** and **3** have more positive redox potentials compared to **2**, **4** and **5**, in accord with the attachment of electron-withdrawing (CF_3) and electron-donating (Bu^t) groups. Comparison between **2** and **5**, where the complexes differ only by the presence of an

additional Bu^t group at the pyridyl group of the phenoxy-containing tridentate chelate in **5**, shows similar oxidation potentials but different reduction potentials by 0.16 V.

Electronic structure calculations on the five Ir(III) complexes **1** - **5** indicate the LUMO to be at both the pyrazolyl and pyridyl unit of 6-pyrazolyl-2-phenoxylpyridine chelate in all cases (Figures 3 and S3, Tables S2 and S3). This is in contrast with the LUMO of **SB** which is located on the same pyridyl unit and with contribution from the fluorophenyl unit as shown in Figure 3.

The HOMOs of **1** - **5** are of mixed metal-ligand character with both the metal d_π orbital and fluorophenoxy ring as the dominant contributor in all except **4** where the HOMO is on the phenyl group of the dicarbene pincer moiety. In turn, the HOMO-1 in **4** has mixed metal-ligand character with electron contribution similar to the HOMO of all other complexes, and is only 0.03 eV lower than HOMO in energy. The HOMO and HOMO-1 are also close in energy for the tert-butyl derivatives **2** and **5**.

The HOMO in **SB** differs from the HOMOs in **1** - **5** where the HOMO in **SB** has contributions from all units of the $pzpyph^F$ chelate (Figure 3). The computed HOMO and LUMO energies for **SB** are identical to those for **1**. This is remarkable as different observed lowest energy absorption bands and emission maxima for these complexes usually reflect different HOMO-LUMO energy gaps (HLGs). Our objective of widening the HLG energy using a non-conjugated chelate was therefore not supported by electronic structure calculations. These computations suggest that absorption and emission energies are not correctly predicted from calculated HLG energies but, as discussed later, are correctly predicted by time-dependent hybrid DFT (TD-DFT) calculations.

The agreement between computed HOMO energies of **1** - **5** and observed oxidation potentials of **1** - **5** from cyclic voltammetry is excellent (Table S2). The

trend between the LUMO energies of **1** - **5** fits well to the reduction wave potentials of **1** - **5**. The observed difference of 0.16 V in the reduction potentials between **2** and **5** is mirrored by the difference of 0.16 V in the LUMO energies of **2** and **5** supporting the fact that the LUMO is mainly on the central pyridyl ring of the dianionic chelate. The electron-withdrawing CF_3 group of dicarbene pincer chelate clearly lower the frontier orbital energies while the electron-donating tert-butyl group raise the frontier orbital energies.

The relationship between the metal contribution in the MLCT excited state and emission lifetime is confirmed by MO computations here. The metal contributions in both HOMO and HOMO-1 are highest for **2** and lowest for **3** (Tables 2, S2 and S3) where **2** and **3** have the shortest and longest observed emission lifetimes, respectively (Table 1). TD-DFT computations on all complexes **1** - **5** and **SB** gave predicted wavelengths in excellent agreement with the observed deep blue emissions from the class of non-conjugated complexes **1** - **5** and the sky-blue emitting **SB** (Table 2). The differences in the emission colors between these complexes are attributed to the different frontier orbital make-ups **1** - **5** and reference **SB** where the oxygen atom breaks up the conjugation of chromophoric chelate in the former complexes.

These characteristics indicate their high potential in fabrication of true-blue emitting OLEDs. Initially we employed 9-(3-(9*H*-carbazol-9-yl)phenyl)-9*H*-carbazole-3-carbonitrile (mCPCN)[14,21,22] as host that has a relatively large triplet gap (E_T) of 2.9 eV, and with characteristics similar to those of the wide triplet gap hosts *N*,*N*-dicarbazolyl-3,5-benzene (mCP) and 4,4'-bis(3-methylcarbazol-9-yl)-2,2'-biphenyl (mCBP) (Figure S4).[5,22] When Ir(III) emitters were doped in mCPCN host (12 wt.%), only complex **2** exhibited a PLQY value comparable to that recorded in solution, while all other complexes (**1**, **3** - **5**) with more blue emissions gave relatively

reduced PLQYs. This is probably associated with a poor host-to-guest energy transfer due to an inefficient host/guest spectral overlap and poor triplet exciton confinement due to the reduced host/guest triplet energy gap (Figure S5). We then turned to bis[2-(diphenylphosphino)phenyl]ether oxide (DPEPO) as host with an even larger triplet gap of E_T of 3.35 eV,[21] in which PLQYs of 81% and 91% and emission lifetimes of 3.83 μs and 3.98 μs were observed for **2** and **5** respectively (Table 1 and Figure S6). Thus the OLEDs were best fabricated using the architecture: ITO/MoO_3 (1 nm)/TAPC (40 nm)/mCP (10 nm)/DPEPO doped with **2** or **5** (12 wt.%, 20 nm)/3TPYMB (50 nm)/LiF (1 nm)/Al (100 nm), for which TAPC, mCP and 3TPYMB stand for 1,1-bis[(di-4-tolylamino)phenyl]cyclohexane, *N*,*N*-dicarbazolyl-3,5-benzene and tris-[3-(3-pyridyl)mesityl]borane, respectively, and served either as the hole- or electron-transport layers (Figure 4).[22] Vacuum-deposited DPEPO thin film doped with **2** or **5** constituted the emitting layer (EML). The HOMO/LUMO levels of -5.33 eV/-2.39 eV for **2** and -5.32 eV/-2.31 eV for **5**, obtained from the electrochemical data and the onset of the absorption/emission spectra, are both within the corresponding energy levels of the DPEPO host.

Figures 5a - 5d shows representative EL characteristics of OLEDs for **2** and **5**, while performance parameters of both devices are summarized in Table S4. The EL spectra are similar to their PL spectra, indicating pure EL from either **2** or **5** and presenting $CIE_{(x,y)}$ coordinates of (0.15, 0.24) and (0.15, 0.17) for **2** and **5**, respectively. The further blue-shifted EL from **5** relative to **2** is again consistent with their PL characteristics. These devices in general exhibit a relatively low turn-on voltage of ~2.5 - 3 V and an operation voltage of 5~5.2 V for a practical brightness of 100 $cd \cdot m^{-2}$. The devices containing **2** and **5** show EL efficiencies of up to (19.7%, 33.5 $cd \cdot A^{-1}$, 26.3 $lm \cdot W^{-1}$) and (20.7%, 28.8 $cd \cdot A^{-1}$, 22.6 $lm \cdot W^{-1}$), respectively. The

superior EQE of **5** (vs. **2**) is consistent with the higher PLQY of **5** in thin films, while lower current and power efficiencies of **5** are mainly associated with its deeper blue emission (vs. **2**). With an EQE of >20% and a $CIE_{(x,y)}$ of (0.15, 0.17) from **5**, to our knowledge, these results represent the best deep blue EL from the bis-tridentate Ir(III) complexes, and they are also comparable to the best blue OLEDs using bis-tridentate Ir(III) complexes recorded at practical brightness of 100 $cd \cdot m^{-2}$. Notably, the EL from **2** and **5** are much blue-shifted vs. the EL from **SB** with an identical architecture as shown in Figures 5a and 5b.

In summary, the deep-blue emitting, bis-tridentate Ir(III) phosphors with emission peak maxima in the region of 470 nm were assembled using both dicarbene pincer ancillary and chromophoric 6-pyrazolyl-2-phenoxylpyridine chelate with a partially interrupted π-conjugation. Hybrid-DFT and TD-DFT computations reveal that this interrupted conjugation changes the nature of the frontier orbitals with respect to the sky-blue emitting **SB** with 6-pyrazolyl-2-phenylpyridine chelate. Furthermore, a good correlation was obtained between the emission lifetime and carbene ancillaries: those with imidazolylidene and tert-butyl substituents (i.e. **2** and **5**) exhibited reduced lifetimes against those with either benzimidazolylidene or CF_3 substituents (i.e. **1**, **3** and **4**), due to the varied MLCT contributions at the lowest energy excited states. Overall, OLEDs with dopants **2** and **5** gave excellent performances in all aspects, and shed light on how to develop similar deep blue-emitting OLED phosphors for future industrial applications.

Supporting Information

Supporting Information is available from the Wiley Online Library or from the author.

Acknowledgements

(HHK, KTC and LRD contributed equally to this work. YC acknowledge the Ministry of Science and Technology, Taiwan for funding, 106-2811-M-007-023.)

Received: ((will be filled in by the editorial staff))

Revised: ((will be filled in by the editorial staff))

Published online: ((will be filled in by the editorial staff))

References

[1] a) L. Xiao, Z. Chen, B. Qu, J. Luo, S. Kong, Q. Gong, J. Kido, *Adv. Mater.* **2011**, *23*, 926-952; b) K. Li, G. S. Ming Tong, Q. Wan, G. Cheng, W.-Y. Tong, W.-H. Ang, W.-L. Kwong, C.-M. Che, *Chem. Sci.* **2016**, *7*, 1653-1673; c) C.-W. Lu, Y. Wang, Y. Chi, *Chem. Eur. J.* **2016**, *22*, 17892-17908.

[2] a) W.-C. Chen, C.-S. Lee, Q.-X. Tong, *J. Mater. Chem. C* **2015**, *3*, 10957-10963; b) T. Fleetham, G. Li, J. Li, *Adv. Mater.* **2017**, *29*, 1601861.

[3] Y. Im, S. Y. Byun, J. H. Kim, D. R. Lee, C. S. Oh, K. S. Yook, J. Y. Lee, *Adv. Funct. Mater.* **2017**, *27*, 1603007.

[4] E. D. Baranoff, B. Curchod, *Dalton Trans.* **2015**, *44*, 8318-8329.

[5] a) X. Yang, X. Xu, G. Zhou, *J. Mater. Chem. C* **2015**, *3*, 913-944; b) Y. Zhang, J. Lee, S. R. Forrest, *Nat. Commun.* **2014**, *5*, 5008; c) J. Lee, H.-F. Chen, T. Batagoda, C. Coburn, P. I. Djurovich, M. E. Thompson, S. R. Forrest, *Nat. Mater.* **2016**, *15*, 92-98.

[6] S. Scholz, D. Kondakov, B. Lüssem, K. Leo, *Chem. Rev.* **2015**, *115*, 8449-8503.

[7] V. L. Whittle, J. A. G. Williams, *Dalton Trans.* **2009**, 3929-3940.

[8] T. Yutaka, S. Obara, S. Ogawa, K. Nozaki, N. Ikeda, T. Ohno, Y. Ishii, K. Sakai, M. Haga, *Inorg. Chem.* **2005**, *44*, 4737-4746.

[9] N. Darmawan, C.-H. Yang, M. Mauro, M. Raynal, S. Heun, J. Pan, H. Buchholz, P. Braunstein, L. De Cola, *Inorg. Chem.* **2013**, *52*, 10756-10765.

[10] R. G. Alabau, B. Eguillor, J. Esler, M. A. Esteruelas, M. Oliván, E. Oñate, J.-Y. Tsai, C. Xia, *Organometallics* **2014**, *33*, 5582-5596.

[11] J. A. Treadway, B. Loeb, R. Lopez, P. A. Anderson, F. R. Keene, T. J. Meyer, *Inorg. Chem.* **1996**, *35*, 2242-2246.

[12] Y. Chi, T.-K. Chang, P. Ganesan, P. Rajakannu, *Coord. Chem. Rev.* **2017**, doi: 10.1016/j.ccr.2016.1011.1016.

[13] a) B. Tong, H. Y. Ku, I. J. Chen, Y. Chi, H.-C. Kao, C.-C. Yeh, C.-H. Chang, S.-H. Liu, G.-H. Lee, P.-T. Chou, *J. Mater. Chem. C* **2015**, *3*, 3460-3471; b) J. Lin, N.-Y. Chau, J.-L. Liao, W.-Y. Wong, C.-Y. Lu, Z.-T. Sie, C.-H. Chang, M. A. Fox, P. J. Low, G.-H. Lee, Y. Chi, *Organometallics* **2016**, *35*, 1813-1824.

[14] C.-Y. Kuei, W.-L. Tsai, B. Tong, M. Jiao, W.-K. Lee, Y. Chi, C.-C. Wu, S.-H. Liu, G.-H. Lee, P.-T. Chou, *Adv. Mater.* **2016**, *28*, 2795-2800.

[15] C.-Y. Kuei, S.-H. Liu, P.-T. Chou, G.-H. Lee, Y. Chi, *Dalton Trans.* **2016**, *45*, 15364-15373.

[16] Y.-H. Song, Y.-C. Chiu, Y. Chi, Y.-M. Cheng, C.-H. Lai, P.-T. Chou, K.-T. Wong, M.-H. Tsai, C.-C. Wu, *Chem. Eur. J.* **2008**, *14*, 5423.

[17] a) C.-F. Chang, Y.-M. Cheng, Y. Chi, Y.-C. Chiu, C.-C. Lin, G.-H. Lee, P.-T. Chou, C.-C. Chen, C.-H. Chang, C.-C. Wu, *Angew. Chem. Int. Ed.* **2008**, *47*, 4542-4545; b) Y.-C. Chiu, J.-Y. Hung, Y. Chi, C.-C. Chen, C.-H. Chang, C.-C. Wu, Y.-M. Cheng, Y.-C. Yu, G.-H. Lee, P.-T. Chou, *Adv. Mater.* **2009**, *21*, 2221-2225; c) Y.-C. Chiu, Y. Chi, J.-Y. Hung, Y.-M. Cheng, Y.-C. Yu, M.-W. Chung, G.-H. Lee, P.-T. Chou, C.-C. Chen, C.-C. Wu, H.-Y. Hsieh, *ACS Appl. Mater. Interfaces* **2009**, *1*, 433-442; d) L. He, L. Duan, J. Qiao, G. Dong, L. Wang, Y. Qiu, *Chem. Mater.* **2010**, *22*, 3535-3542; e) C.-H. Yang, M. Mauro, F. Polo, S. Watanabe, I. Muenster, R. Fröhlich, L. De Cola, *Chem. Mater.* **2012**, *24*, 3684-3695; f) Y. Kang, Y.-L. Chang, J.-S. Lu, S.-B. Ko, Y. Rao, M. Varlan, Z.-H. Lu, S. Wang, *J. Mater. Chem. C* **2013**, *1*, 441-450; g) F. Kessler, Y. Watanabe, H. Sasabe, H. Katagiri, M. K. Nazeeruddin, M. Grätzel, J. Kido, *J. Mater. Chem. C* **2013**, *1*, 1070-1075; h) S. Lee, S.-O. Kim, H. Shin, H.-J. Yun, K. Yang, S.-K. Kwon, J.-J. Kim, Y.-H. Kim, *J. Am. Chem. Soc.* **2013**, *135*, 14321-14328; i) J. Frey, B. F. E. Curchod, R. Scopelliti, I. Tavernelli, U. Rothlisberger, M. K. Nazeeruddin, E. Baranoff, *Dalton Trans.* **2014**, *43*, 5667-5679; j) K. S. Bejoymohandas, A. Kumar, S. Varughese, E. Varathan, V. Subramanian, M. L. P. Reddy, *J. Mater. Chem. C* **2015**, *3*, 7405-7420; k) T. Duan, T.-G. Chang, Y. Chi, J.-Y. Wang, Z.-N. Chen, W.-Y. Hung, C. H. Chen, G.-H. Lee, *Dalton Trans.* **2015**, *44*, 14613-14624; l) J.-H. Lee, G. Sarada, C.-K. Moon, W. Cho, K.-H. Kim, Y. G. Park, J. Y. Lee, S.-H. Jin, J.-J. Kim, *Adv. Opt. Mater.* **2015**, *3*, 211-220; m) T.-Y. Li, X. Liang, L. Zhou, C. Wu, S. Zhang, X. Liu, G.-Z. Lu, L.-S. Xue, Y.-X. Zheng, J.-L. Zuo, *Inorg.*

Chem. **2015**, *54*, 161-173; n) Y.-H. Kim, J.-B. Kim, S.-H. Han, K. Yang, S.-K. Kwon, J.-J. Kim, *Chem. Commun.* **2015**, *51*, 58-61; o) Y. Nagai, H. Sasabe, S. Ohisa, J. Kido, *J. Mater. Chem. C* **2016**, *4*, 9476-9481; p) Y. Feng, X. Zhuang, D. Zhu, Y. Liu, Y. Wang, M. R. Bryce, *J. Mater. Chem. C* **2016**, *4*, 10246-10252; q) Y.-J. Cho, S.-Y. Kim, J.-H. Kim, J. Lee, D. W. Cho, S. Yi, H.-J. Son, W.-S. Han, S. O. Kang, *J. Mater. Chem. C* **2017**, *5*, 1651-1659.

[18] V. C. Vargas, R. J. Rubio, T. K. Hollis, M. E. Salcido, *Org. Lett.* **2003**, *5*, 4847-4849.

[19] D. Maiti, S. L. Buchwald, *J. Org. Chem.* **2010**, *75*, 1791-1794.

[20] L. Hammarström, F. Barigelletti, L. Flamigni, M. T. Indelli, N. Armaroli, G. Calogero, M. Guardigli, A. Sour, J.-P. Collin, J.-P. Sauvage, *J. Phys. Chem. A* **1997**, *101*, 9061-9069.

[21] a) Q. Zhang, B. Li, S. Huang, H. Nomura, H. Tanaka, C. Adachi, *Nat. Photon.* **2014**, *8*, 326-332; b) Y.-J. Hsu, Y.-T. Chen, W.-K. Lee, C.-C. Wu, T.-C. Lin, S.-H. Liu, P.-T. Chou, C.-W. Lu, I. C. Cheng, Y.-J. Lien, Y. Chi, *J. Mater. Chem. C* **2017**, *5*, 1452-1462.

[22] a) M.-S. Lin, S.-J. Yang, H.-W. Chang, Y.-H. Huang, Y.-T. Tsai, C.-C. Wu, S.-H. Chou, E. Mondal, K.-T. Wong, *J. Mater. Chem.* **2012**, *22*, 16114-16120; b) W.-L. Tsai, M.-H. Huang, W.-K. Lee, Y.-J. Hsu, K.-C. Pan, Y.-H. Huang, H.-C. Ting, M. Sarma, Y.-Y. Ho, H.-C. Hu, C.-C. Chen, M.-T. Lee, K.-T. Wong, C.-C. Wu, *Chem. Commun.* **2015**, *51*, 13662-13665.

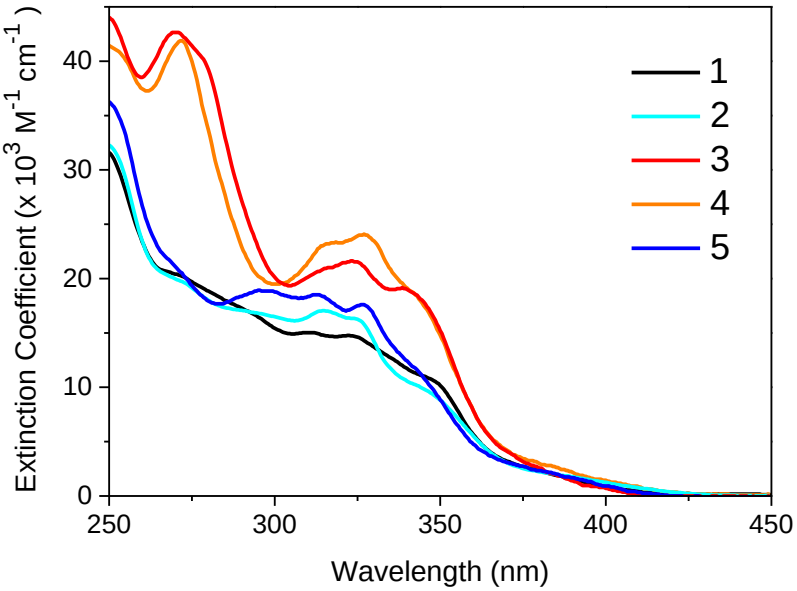

Figure 1. Absorption spectra of Ir(III) complexes **1** – **5** recorded in CH_2Cl_2 at RT.

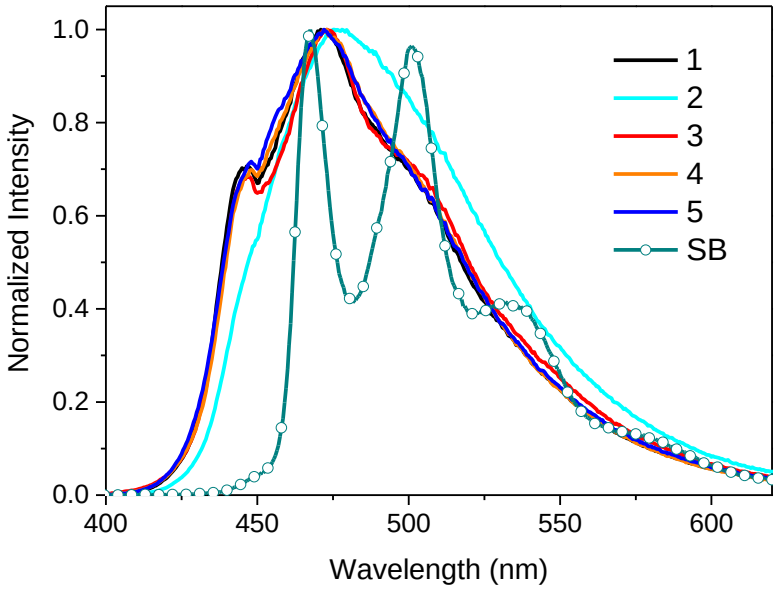

Figure 2. Normalized emission spectra of Ir(III) complexes **1** – **5** and **SB** recorded in degassed CH_2Cl_2 at RT.

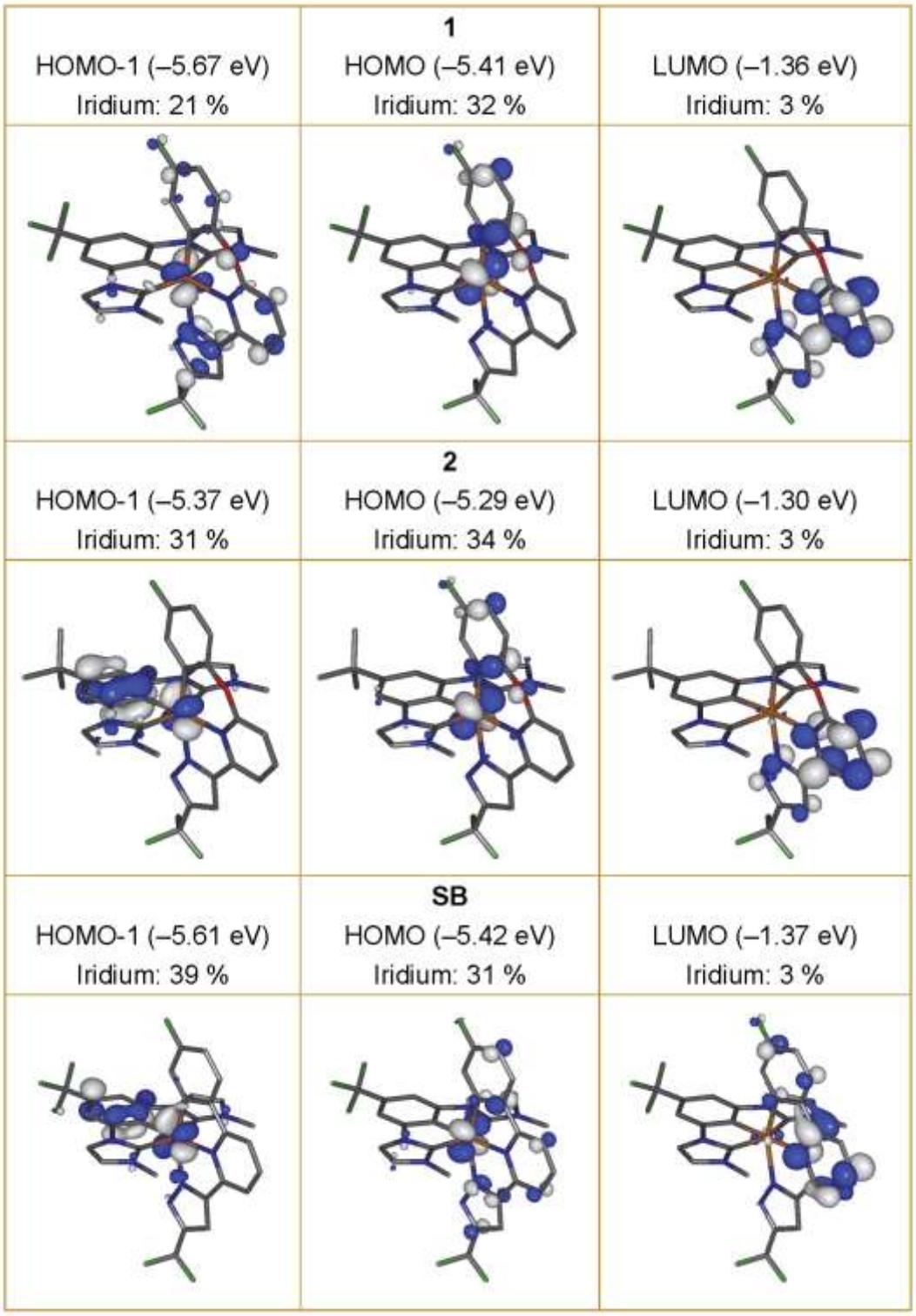

Figure 3. Plots of the frontier orbitals for Ir(III) complexes **1**, **2** and **SB** with MO energies and % iridium MO contributions. All contours are plotted at ±0.06 $(e/bohr^3)^{1/2}$. All hydrogen atoms are omitted for clarity.

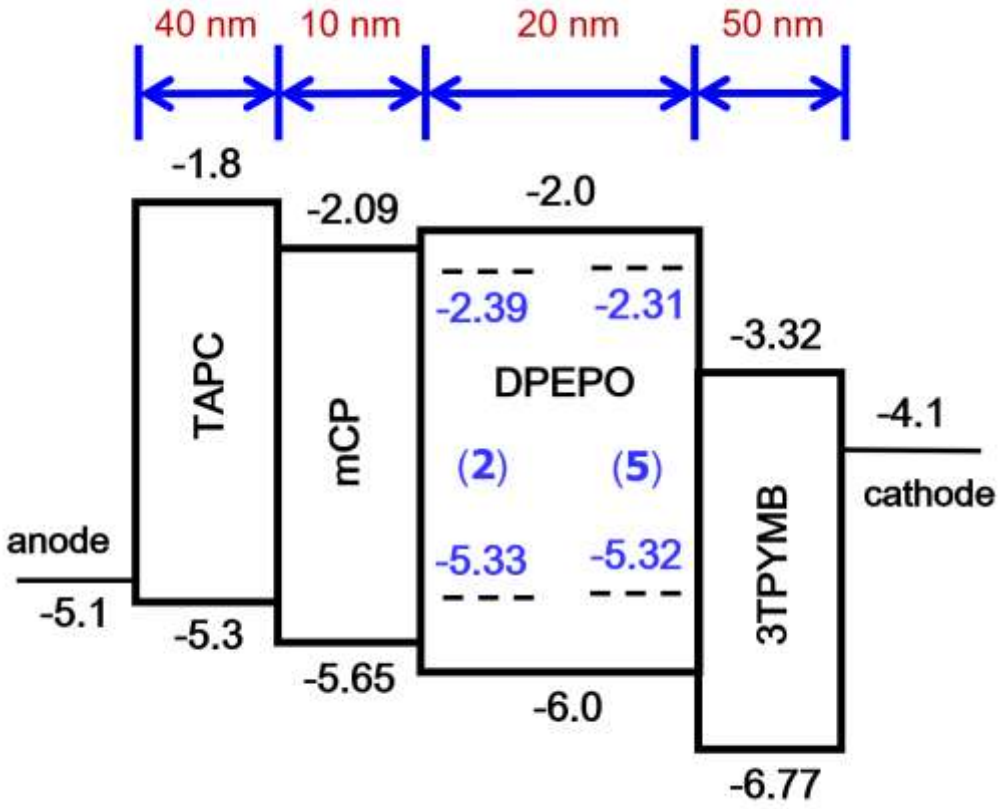

Figure 4. Device configuration and relative energy levels of materials used in OLEDs.

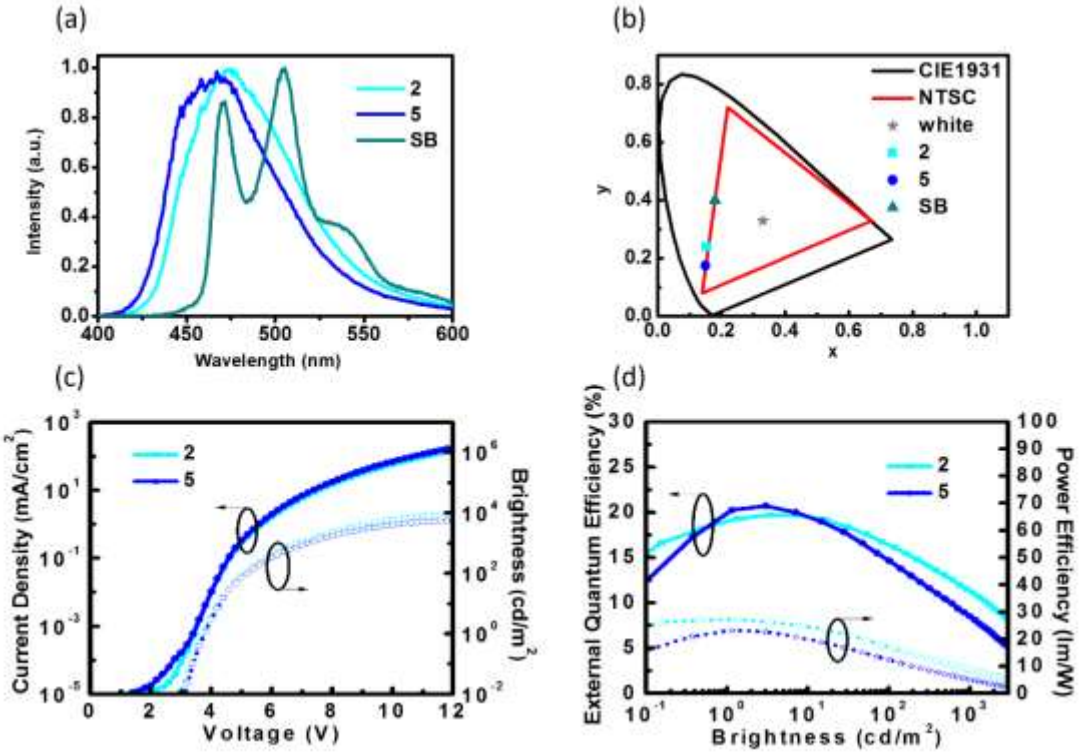

Figure 5. (a - b) EL spectra and 1931 $CIE_{(x,y)}$ coordinates, for which the respecitve data for **SB** are also included; (c) current-voltage-luminance (I-V-L) characteristics and (d) external quantum efficiencies (EQEs) and power efficiencies of devices **2** and **5** at the doping conc. of 12 wt.%.

Table 1. Photophysical and electrochemical data of the studied Ir(III) phosphors **1** – **5**.

	abs λ_{max} [nm] (ε [$\times 10^{-3}$ M^{-1} cm^{-1}])[(a)]	PL λ_{max} [nm][(a)]	FWHM[(b)]	Φ [%][(a)]	τ_{obs} [µs][(a)]	$E^{ox}_{½}$ [V] (ΔE_p, V)[(c)]	E^{re}_{pc} [V][(d)]
1	323 (14.7), 348 (10.6), 384 (2.0), 418 (0.2)	447 (sh), 471, 505 (sh)	3700	81	25.1	0.67 (0.08)	-2.92
2	326 (16.1), 349 (9.1), 388 (1.9), 420 (0.4)	444, 478, 505 (sh)	3500	82/81[(e)]	4.42/3.83[(e)]	0.53 (0.07)	-2.94
3	323 (21.6), 345 (17.8), 387 (1.8), 404 (0.4)	447 (sh), 473, 506 (sh)	3330	68	61.2	0.80 (0.08)	-2.80
4	326 (24.0), 345 (17.5), 387 (2.4), 419 (0.4)	448 (sh), 473, 506 (sh)	3670	79	18.6	0.62 (0.07)	-2.94
5	327 (17.5), 346 (10.2), 386 (1.8), 412 (0.3)	448 (sh), 472, 505 (sh)	3500	72/91[(e)]	8.66/3.98[(e)]	0.52 (0.08)	-3.10

(a) UV-Vis spectra, PL spectra, lifetime and quantum yields were recorded in CH_2Cl_2 at a conc. of 10^{-5} M.

(b) FWHM: full width at half maxima of PL emission in cm^{-1}.

(c) $E^{ox}_{½}$ refers to [(E_{pa} + E_{pc})/2], where E_{pa} and E_{pc} are the anodic and cathodic wave respectively, for the oxidation half-wave potential and referenced to the ferrocene redox couple (FcH/FcH^+ = 0 V), $\Delta E_p = E_{pa} - E_{pc}$ conducted in CH_2Cl_2 solution.

(d) E^{re} is the cathodic wave potential for the irreversible reduction wave referenced to the ferrocene redox couple (FcH/FcH^+ = 0 V) in THF solution.

(e) PLQYs and excited-state lifetimes when doped in thin films of the host material DPEPO.

Table 2. Calculated metal MO contributions and $S_0 \rightarrow S_1$, $S_0 \rightarrow T_1$ and $S_0 \leftarrow T_1$ transition energies (in nm) for **1** – **5** and **SB** with observed absorption (abs) and emission (em) maxima included for comparison.

	%Ir[(a)]	$S_0 \rightarrow S_1$	oscillator strength (*f*)	observed[(b)] λ_{max} (abs)	$S_0 \rightarrow T_1$	observed[(c)] λ_{max} (abs)	$S_0 \leftarrow T_1$	observed[(d)] λ_{max} (em)
1	27	368	0.0132	384	418	418	445	447
2	33	375	0.0096	388	417	420	444	448
3	26	362	0.0277	387	424	404	451	447
4	27	366 368 ($S_0 \rightarrow S_2$)	0.0020 0.0185	387	423	419	450	448
5	32	365	0.0136	386	412	412	438	448
SB	35	380	0.0243	401	442	431	470	467

(a) From HOMO-1 and HOMO. (b) ^{1}MLCT band. (c) ^{3}MLCT band. (d) Highest energy emission maximum.

The table of contents entry should be 50−60 words long,

A deep-blue OLED from one bis-tridentate Ir(III) phosphor **5** exhibit $CIE_{(x,y)}$ of (0.15, 0.17) with max. EQE of 20.7% and EQE = 14.6% at the practical brightness of 100 $cd \cdot m^{-2}$.

Keyword

iridium, phosphorescence, organic light emitting diode, carbene, pyrazole, tridentate

Author

Hsin-Hung Kuo,[a,‡] Yi-Ting Chen,[b,‡] Leon R. Devereux,[c,‡] Chung-Chih Wu,[b,] Mark A. Fox,[c,]* Chu-Yun Kuei,[a] Yun Chi,[a,]* and Gene-Hsiang Lee[d]*

Title

Bis-tridentate Ir(III) Metal Phosphors for Efficient Deep-Blue Organic Light-Emitting Diodes